International Journal of Modern Manufacturing Technologies
ISSN 2067–3604, Vol. X, No. 1 / 2018

AN EXPERIMENTAL STUDY ON DEEP HOLE MACHINING IN BRASS USING ABRASIVE WATER JET MACHINE

Bhaskar Govindasamy Bhavani[1], Guru Prasath Muthukrishanan Yoga[2], Mohana Sundaram Ramasubramania[3], Arun Kumarr Balaji[4], Selva Kumar Mariappan[5], Lenin Raj Sundarajan[6], Varatharajan Rajagopalan[7]

[1,2,3,4,5,6] Department of Production Technology, MIT-Anna University, Chennai, 400 feet Outer Ring Road, Avadi, 600062 TamilNadu, India
[7] Department of Mechanical Engineering, Veltech Dr.RR &Dr.SR University, Chennai, 400 feet Outer Ring Road, Avadi, 600062 TamilNadu, India.

Corresponding author: Varatharajan Rajagopalan, drvaratharajan@veltechuniv.edu.in

Abstract: Production of higher quality deep holes, with kerf minimization, is a challenge in employing abrasive water jet (AWJ) technique. Owing to various distinct advantages, deep hole making accomplished using AWJ machining is preferred over conventional methods. In the recent decades, some of the AWJ machining technologies such as AWJ milling, AWJ turning and AWJ polishing have gradually become mature and steady. However, a few investigations on AWJ deep hole making for the machining of ductile materials had been reported. In this study, an attempt has been made to produce accurate deep holes by optimizing the input parameters viz. water jet pressure, stand-off-distance and abrasive mass flow rate. Experiments are conducted on brass 353 to study the effect of input parameters on material removal rate, surface roughness and kerf quality. Taguchi L18 orthogonal array is adopted and an optimal combination of parameter levels is obtained using Taguchi based Grey relational analysis. Further, the hole is machined with optimal parameter levels and whole correction time is found out by permitting excess piercing to obtain near perfect holes.

Key words: abrasive, kerf, deep hole machining, surface roughness, water jet pressure.

1. INTRODUCTION

Abrasive water jet (AWJ) machining is one of the recent non-traditional methods that has been used widely in industry in many applications including hole making in ductile materials such as aluminium, brass, steel, titanium, and nickel based alloys as well as brittle materials like glass, stone, and ceramics [1]. It has various distinct advantages over the other non-traditional cutting technologies, such as no thermal distortion, high machining versatility, minimum stresses on the work piece, high flexibility and small cutting forces. It is superior to many other cutting techniques in processing variety of materials and has found extensive applications in industry [2]. AWJ machining technology has received considerable attention from industry because of the beneficial characteristics of material removal. This technology can achieve faster machining speeds and leave a fine surface quality free of thermal distortion [3-4]. However, the major obstructions that limit its application are the depth of cut and kerf quality [5]. A great deal of research has been done to improve the cutting performance and enhance the cutting capacity of AWJ cutting technology, including studies of the mechanism of the AWJ cutting process [6-8] and modelling for process control and optimization [9-12]. The material removal mechanism, the machined surface characteristics and the effect of process parameters on machined surface quality have been studied in greater detail [13-15]. The AWJ drilling is a process used frequently in industry by which small-diameter holes can be machined expediently. It is critically important to control the size and shape of the hole and the quality of surfaces in drilling process by AWJ. Some studies have revealed some of the drilling mechanisms [16-17]. By controlling the jet's pressure-time profile and the abrasive flow rate, it is proved that the hole of high quality can be drilled by AWJ. An attempt to minimize the damage to various materials during hole drilling is accomplished by replacing AWJ with cryogenic jets/abrasive cryogenic jets and concluded that the latter method is more expensive and hazardous. An attempt to increase material removal rate is made by carrying out machining in the presence of chemically active liquids such as acetone and phosphoric acid rather than plain water in the slurry and the material removal was identified to be the highest in the case of slurry mixed with polymer (polyacrylamide) rather than other two chemical environments. An experimental investigation to study the effect of parameters such as water pressure, traverse speed and stand-off distance using Abrasive Water Jet Machine (AWJM) for glass/epoxy Composite surfaces was carried out and found that the type of abrasive material is the

most significant factor on surface roughness (SR). Experiments conducted to study the influence of process parameters on depth of cut in abrasive water-jet cutting of mild steel reveals that standoff distance has no apparent effect on depth of cut. Drilling by AWJM does not significantly affect the micro structure and mechanical properties of the material.

Brass is widely used in deep hole micro machining for the manufacture of pneumatic hosing, hydraulic fittings etc. Economic machining of brass is the need of the hour for the mass production of components such as heating, ventilation and air condition (HVAC) appliances, temperature sensors, air brake hose fitting. Deep holes of small diameter (d < 4mm) and high aspect ratio (l/d < 20) still remains a challenge in manufacturing domain.

In the recent decades, much importance has been given to improve AWJ machining technologies. Some of the processes attracted greater attention such as AWJ milling, AWJ turning, AWJ drilling have gradually become mature and steady. However, a few investigations on AWJ deep hole making for the machining of ductile materials had been reported.

In the current study, an attempt has been made to study the influence of process parameters on crucial output responses like SR, Kerf angle and MRR. The results show that, a near perfect deep hole can be machined when excess time for hole-correction is permitted after piercing.

2. MATERIAL

In this study, brass 353 block of 60mm x 50mm x 50mm is utilized for the purpose of deep hole machining. The composition of work specimen reveals the following: copper (60-63)%, zinc (34.5-39)%, lead (1.50-2.50)% and iron 0.10%. The following figure 1 shows the block of brass -353 used in this study.

Fig. 1. Brass specimen used in this study

3. SCHEMATIC OF MACHINING

The machine and pump was switched on. Wait until the water reaches the stable temperature. The machine was connected with the computer for the operation to take place. In the software the cut quality, starting point, material thickness, and material type were given. Dry run was done to make sure that the machine was connected to the computer. The pressure and other conditions were fixed. The component was mounted and fixed properly before machining. The pressure was varied just by operating the pump without abrasives. The stand-off distance was fixed on the computer itself. The abrasives of proper size were filled in the abrasive hopper. The above same experiments were performed on brass and the respective time of piercing was noted. After the experiment the 50mm block was sectioned into 5 parts of each 10mm thickness and the top diameter and bottom diameter were measured in video measurement system. The kerf angle, kerf width, SR and MRR were calculated for each hole. The optimal parametric combination for minimum standard deviation, minimum range and minimum time was found using grey relational analysis and compared with Minitab software result.

4. DESIGN OF EXPERIMENTS

The parameters and levels were selected based on the literature review of some studies that had been documented on AWJ machining on graphite/epoxy laminates [5], metallic coated sheet steels [8] and fiber-reinforced plastics [14]. Taguchi's experimental design was used to construct the design of experiments (DOE). Three process parameters, i.e. water pressure varied at six levels, stand-off distance (SOD) and abrasive mass flow rate mass flow rate each varied at three levels as shown in Table 1, an L18 orthogonal arrays table with 18 rows corresponding to the number of experiments was selected for the experimentation. The input parameters and their levels selected are tabulated in Table 1. The Taguchi L18 Orthogonal design for selected factors is tabulated in Table 2. The machined holes are sectioned into five parts of 10mm each and their depth averaged diameter (top and bottom diameter) are measured and the standard deviation and range are calculated.

Table 1. The factors with different level values

Parameters	Level					
	1	2	3	4	5	6
Pressure [MPa]	245	254	267	281	295	309
SOD [mm]	2	3	4	-	-	
Abrasive Mass Flow Rate	185	289	432	-	-	-

5. RESULTS AND DISCUSSION

5.1. Data collection

The holes were machined with the combination of parameter levels as specified in the Table 2 and the piercing time is noted. The weight of the work piece

before machining and after machining are noted and MRR in terms of volume is calculated by using the formula, MRR= Weight Removed/ Piercing Time × Density of the material.

Table 2. L 18 Taguchi Orthogonal Design for selected factors

S. No	Pressure [MPa]	SOD [mm]	AMFR [g/min]	Hole ID
1	247	2	185	H1
2	247	3	289	H2
3	247	4	432	H3
4	254	2	185	H4
5	254	3	289	H5
6	254	4	432	H6
7	267	2	289	H7
8	267	3	432	H8
9	267	4	185	H9
10	281	2	432	H10
11	281	3	185	H11
12	281	4	289	H12
13	295	2	289	H13
14	295	3	432	H14
15	295	4	185	H15
16	309	2	432	H16
17	309	3	185	H17
18	309	4	289	H18

Work piece surface roughness Ra was measured by a contact type surface roughness Profilometer model "SE 3500" with the resolution of 0.1 Nm, measuring range of 600 µm. Surface roughness was measured at the centre of the cut for each specimen and the values are tabulated. The holes were sectioned into five pieces each of thickness 10mm, along its depth. The holes were examined with VMS of resolution and accuracy 0.001mm and +/- 3µm. The readings were taken for five times and they were averaged. With the readings of diameter values taken for each hole, the hole profiles are plotted in Figure 8, Figure 9, Figure 10. The kerf angles for L18 Orthogonal design are shown in Table 3. The material removal rates for L18 Orthogonal design are shown in Table 4. The mean, standard deviation and range of each hole are tabulated in Table 5.

5.2. Parameter Optimization

The goal of this study is to find out the optimum set of parameter levels so as to achieve optimized results while machining in AWJM. So our requirement is to minimize the kerf angle of each hole, minimize the surface roughness and maximize the material removal rate. The found optimized level of combination is employed to make deep holes to estimate the hole correction time. The optimization was done using Grey rational analysis, Taguchi based Grey Rational Analysis and using MINITAB software and the results were compared.

5.3. MINITAB method

The plot from MINITAB software is established in Figure 2 and the optimal combination level is shown in Figure 3. The Figure 4 shows the optimization plot for means. The Figure 5 shows the mean effects plot for S/N ratios.

The optimal combination predicted by Minitab Software is: AMFR = 185g/min; Water Pressure = 281 MPa; SOD = 3mm.

The reason for low composite desirability is due to the interaction effects are not accommodated in the model.

Table 3. Kerf angles for L18 Orthogonal Design

Hole ID	Top diameter (D1) [mm]	Bottom diameter (D2) [mm]	Kerf width [mm]	Kerf angle [deg]
H1	2.083	1.774	0.309	0.177043
H2	2.174	0.805	1.369	0.78433
H3	2.339	0.815	1.524	0.87312
H4	2.107	1.29	0.817	0.468096
H5	2.236	0.854	1.382	0.791777
H6	2.395	1.244	1.151	0.659445
H7	2.177	0.929	1.248	0.715014
H8	2.286	0.88	1.406	0.805526
H9	2.192	0.862	1.33	0.761989
H10	2.226	0.871	1.355	0.77631
H11	2.094	1.665	0.429	0.245797
H12	2.285	0.888	1.397	0.80037
H13	2.132	1.553	0.579	0.331739
H14	2.262	1.886	0.376	0.215431
H15	2.195	0.749	1.446	0.828439
H16	2.234	0.82	1.414	0.810108
H17	2.14	0.858	1.282	0.734492
H18	2.169	0.801	1.368	0.783757

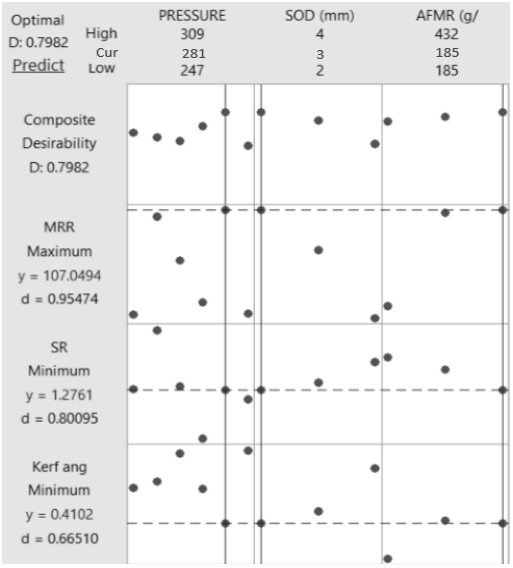

Fig. 2. Optimization plot

Moreover, the individual desirability of the kerf angle is 0.66, which lowers the composite desirability to 0.7982. Hence, it could be inferred that the present set of parameter levels is more promising to achieve the optimal SR and MRR except for the kerf angle.

Grey relational analysis:

1. The higher the better

xi*(k)=(xi(0)(k) – min xi(0)(k))/(max xi(0)(k) – min xi(0)(k))

2. The lower the better

xi*(k)=(max xi(0)(k) – xi(0)(k))/(max xi(0)(k) – min xi(0)(k))

The Grey relational coefficient is defined as follows:

$$\zeta i\ (k) = (\Delta min + \zeta \Delta max)/(\ (\Delta oi\ (k) + \zeta \Delta max)$$

Response Optimization: MRR, SR, Kerf angle

Parameters

Response	Goal	Lower	Target	Upper	Weight	Importance
MRR	Maximum	50.4009	109.735		1	1
SR	Minimum		0.880	2.87000	1	1
Kerf angle	Minimum		0.177	0.87312	1	1

Solution

Solution	PRESSURE (MPa)	SOD (mm)	AFMR (g/min)	MRR Fit	SR Fit	Kerf angle Fit	Composite Desirability
1	281	3	185	107.049	1.27611	0.410158	0.798228

Multiple Response Prediction

Variable	Setting
PRESSURE (MPa)	281
SOD (mm)	3
AFMR (g/min)	185

Response	Fit	SE Fit	95% CI	95% PI
MRR	107.0	10.7	(82.4, 131.7)	(65.7, 148.4)
SR	1.276	0.362	(0.441, 2.111)	(-0.121, 2.674)
Kerf angle	0.410	0.180	(-0.004, 0.824)	(-0.283, 1.103)

Fig. 3. Optimization result

Table 4. MRR L18 orthogonal design

Hole ID	SR [µm]	Piercing Time [s]	Weight before machining [g]	Weight after machining [g]	Weight removed [g]	Material removed/unit time [g/min]	MRR [mm^3/min]
H1	1.55	158	956	954.5	1.5	0.5696	65.2485972
H2	1.29	145	947.4	945.5	1.9	0.7862	90.0580638
H3	1.96	143	936.7	935.4	1.3	0.5455	62.4804749
H4	2.1	152	954.5	952.5	2	0.7895	90.4322662
H5	2.87	143	945.5	943.7	1.8	0.7552	86.5114267
H6	1.72	137	935.4	933.5	1.9	0.8321	95.3169288
H7	1.28	133	943.7	941.8	1.9	0.8571	98.1836033
H8	1.03	123	933.5	932	1.5	0.7317	83.8152711
H9	2.56	146	952.5	951.1	1.4	0.5753	65.9040625
H10	0.96	153	932	930.4	1.6	0.6275	71.8729645
H11	0.88	140	951.1	949.7	1.4	0.6	68.7285223
H12	1.36	123	941.8	940.3	1.5	0.7317	83.8152711
H13	1.61	119	939.7	937.8	1.9	0.958	109.734616
H14	1.46	113	930.4	928.7	1.7	0.9027	103.396892
H15	1.7	132	949.7	948.5	1.2	0.5455	62.4804749
H16	1.34	105	928.7	987.1	1.6	0.9143	104.729177
H17	1.78	120	948.5	947.4	1.1	0.55	63.0011455
H18	1.34	150	937.8	936.7	1.1	0.44	50.40091638

Where Δoi (k) is the deviation sequence of the reference sequence xo*(k) and the comparability sequence is xi*(k), ζ distinguishing or identification coefficient. If all the parameters are given equal preference, ζ is taken as 0.5.

The Grey relational grade is defined as follows:

$$\gamma i = (1/n)\ \Sigma \zeta i\ (k)$$

Where γi is the Grey relational grade for the ith experiment and n is the number of performance characteristic.

5.4. Grey relational analysis on making deep holes

As our objective is to minimize standard deviation, range and time, we are using smaller the better formula to find the normalized values.

$$Xi^*(k) = (\max xi(0)(k) - xi(0)(k))/(\max xi(0)(k) - \min xi(0)(k))$$

Once the normalized values are found, then the Grey relational coefficient is found using the formula,

$$\zeta i\ (k) = (\Delta min + \zeta \Delta max)/(\ (\Delta oi\ (k) + \zeta \Delta max).$$

Table 5. Mean, standard deviation and range of diameter

Hole No	Mean Diameter, [mm]	RMS	Standard deviation	Maximum Diameter, [mm]	Minimum Diameter, [mm]	Range [mm]
H1	2.0833158	2.783	0.388354649	2.38	1.78	1.247
H2	2.1740526	2.772	0.367325318	2.279	2.07	1.149
H3	2.3395789	3.231	0.345750793	2.53	2.13	1.074
H4	2.1076316	2.595	0.35879598	2.508	1.755	1.053
H5	2.2364737	2.845	0.307278195	2.489	2.037	1.012
H6	2.3951579	3.021	0.27533525	3.707	2.839	0.868
H7	2.1770526	2.9	0.283828097	3.826	2.92	0.906
H8	2.2863158	3.089	0.365788949	3.991	2.792	1.199
H9	2.1923684	2.79	0.289479322	3.711	2.79	0.921
H10	2.2268421	2.726	0.345619894	3.905	2.713	1.192
H11	2.0948947	2.591	0.346233784	3.948	2.767	1.181
H12	2.2856842	3.185	0.398906213	3.854	2.457	1.397
H13	2.1323158	2.531	0.324505778	3.898	2.836	1.062
H14	2.2625263	2.864	0.321511361	3.888	2.813	1.075
H15	2.1954737	2.899	0.324707817	3.922	2.856	1.066
H16	2.2345263	2.633	0.290383559	3.908	2.998	0.91
H17	2.147368	3.046	0.299602885	3.926	3.02	0.906
H18	2.1693684	2.761	0.27408099	3.826	2.988	0.838

After the Grey relational coefficient is found, the Grey relation grade is calculated using the formula,

$$\gamma i = (1/n)\ \Sigma \zeta i\ (k)$$

After the grade is found, the mean of Grey relational grade is calculated for each input parameter and the optimal combination is found. The normalized output responses are tabulated in Table 6. The Δ values for the output responses are tabulated in Table 7. The averaged grey relational coefficients and the grey grade for output responses are tabulated in Table 8.

Table 6. The normalized output responses

Hole ID	Kerf	SR [μm]	MRR [mm^3/min]
H1	1	0.66331658	0.74976
H2	0.127558	0.79396985	0.331625
H3	0	0.45728643	0.796413
H4	0.581867	0.38693467	0.325318
H5	0.116859	0	0.3914
H6	0.30697	0.57788945	0.242993
H7	0.227139	0.79899497	0.194679
H8	0.097108	0.92462312	0.43684
H9	0.159654	0.15577889	0.738713
H10	0.139079	0.95979899	0.638114
H11	0.901226	1	0.69111
H12	0.104515	0.75879397	0.43684
H13	0.777761	0.63316583	0
H14	0.944851	0.70854271	0.106815
H15	0.06419	0.5879397	0.796413
H16	0.090524	0.76884422	0.084361
H17	0.199157	0.54773869	0.787638
H18	0.128381	0.76884422	1

5.5. Taguchi based Grey rational analysis

This method of obtaining optimized set of parameter values is same as that of Grey rational analysis with the exemption that the S/N ratio for grey rational grade is calculated and taken into consideration for the selection of parameter set and tabulated. The following Table 9 shows Grey relational grades with corresponding S/N ratios.

Table 7. The Δ values for the output responses

Hole ID	Deviation coefficient		
	Δ Kerf	Δ SR	Δ MRR
H1	0	0.336683	0.25024
H2	0.8724424	0.20603	0.668375
H3	1	0.542714	0.203587
H4	0.4181331	0.613065	0.674682
H5	0.883141	1	0.6086
H6	0.6930298	0.422111	0.757007
H7	0.7728614	0.201005	0.805321
H8	0.9028922	0.075377	0.56316
H9	0.8403464	0.844221	0.261287
H10	0.8609208	0.040201	0.361886
H11	0.0987736	0	0.30889
H12	0.8954855	0.241206	0.56316
H13	0.2222391	0.366834	1
H14	0.0551487	0.291457	0.893185
H15	0.9358104	0.41206	0.203587
H16	0.9094758	0.231156	0.915639
H17	0.8008432	0.452261	0.212362
H18	0.8716194	0.231156	0

Taguchi based Grey Relational Analysis result

From the Table 10, we can observe that the level 4, level 1 and level 2 have the minimum S/N ratio for averaged grey relational coefficient for pressure, AFMR and SOD. So the optimum parametric combination level predicted from Grey Relational Analysis (GRA) is 1) AMFR = 185g/min; 2) Water Pressure = 281MPa; 3) SOD = 3mm.

The above result is similar to that of the result obtained from Minitab Software and that of conventional GRA analysis. The grey relational analysis result is tabulated in the Table 10. The Figure 6 shows the kerf angle variations.

Table 8: The averaged grey relational coefficients and the grey grade for output responses

Hole ID	Grey rational coefficient			Grey rational grade
	Kerf	SR	MRR	
H1	1	0.597598	0.666453	0.754684
H2	0.364314	0.708185	0.427945	0.500148
H3	0.333333	0.479518	0.710644	0.507832
H4	0.544583	0.44921	0.425647	0.473147
H5	0.361496	0.333333	0.451019	0.38195
H6	0.419101	0.542234	0.39777	0.453035
H7	0.392816	0.713262	0.383047	0.496375
H8	0.356407	0.868996	0.470296	0.565233
H9	0.373038	0.371963	0.656782	0.467261
H10	0.367398	0.925581	0.580123	0.624368
H11	0.83504	1	0.618131	0.817724
H12	0.358298	0.674576	0.470296	0.501057
H13	0.692292	0.576812	0.333333	0.534145
H14	0.90066	0.631746	0.35889	0.630432
H15	0.348235	0.548209	0.710644	0.535696
H16	0.354742	0.683849	0.353197	0.463929
H17	0.384366	0.525066	0.70189	0.537107
H18	0.364533	0.683849	1	0.682794

Table 9. Grey relational grades with corresponding S/N ratios

Hole ID	GRG	S/N Ratio
H1	0.754684	-2.4447
H2	0.500148	-6.01803
H3	0.507832	-5.8856
H4	0.473147	-6.50008
H5	0.38195	-8.35988
H6	0.453035	-6.87736
H7	0.496375	-6.0838
H8	0.565233	-4.95545
H9	0.467261	-6.60881
H10	0.624368	-4.09119
H11	0.817724	-1.74787
H12	0.501057	-6.00226
H13	0.534145	-5.44681
H14	0.630432	-4.00724
H15	0.535696	-5.42163
H16	0.463929	-6.67096
H17	0.537107	-5.39878
H18	0.682794	-3.31421
AVERAGE	0.551495	-5.32415

5.6 Graphical interpretation

5.6.1 Graphical interpretation of the effect of pressure, AMFR and SOD on

The Figure 7 shows the MRR variations. The Figure 8 shows the SR variations. From the above graph it is observed that as the AMFR increases, SR decreases linearly, then as the pressure increases, irregular pattern of change is observed and as the SOD increases, SR increases monotonically.

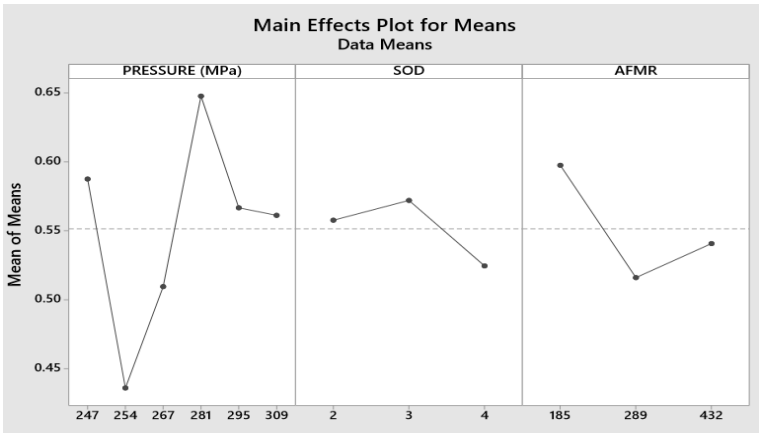

Fig. 4. Optimization plot for means

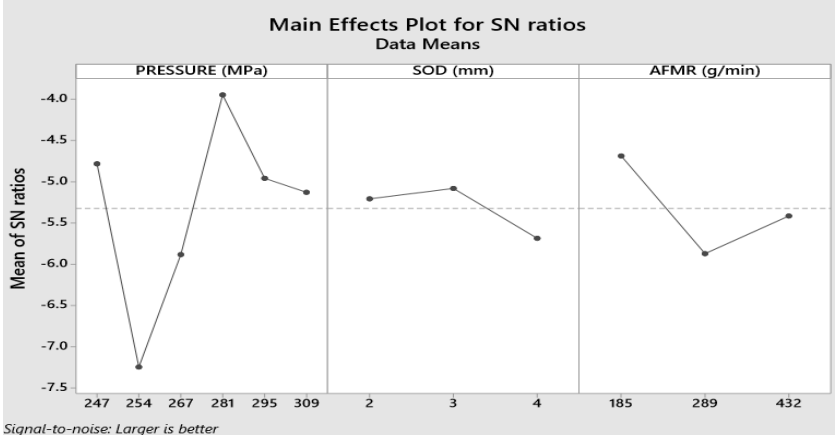

Fig. 5. Optimization plot for S/N ratios

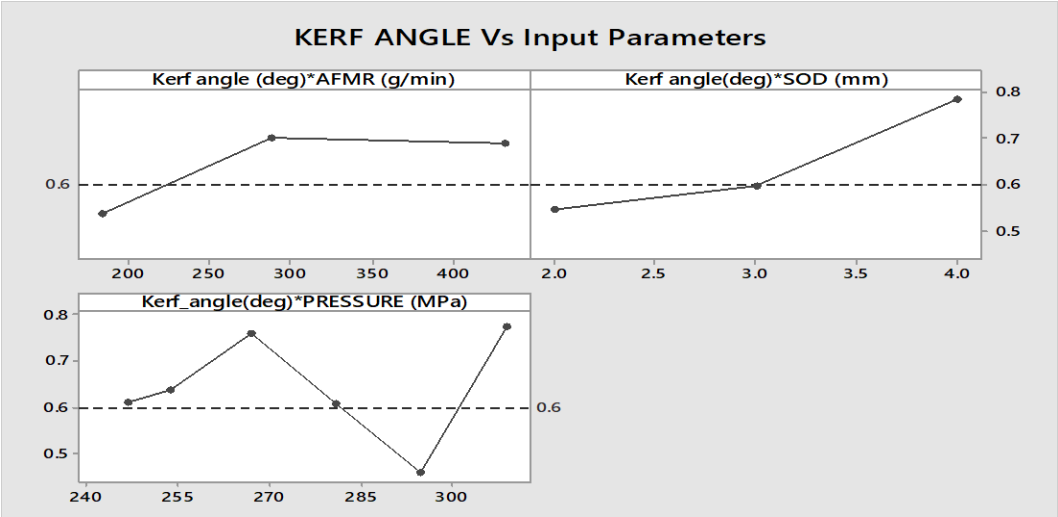

Fig. 6. Kerf angle variations

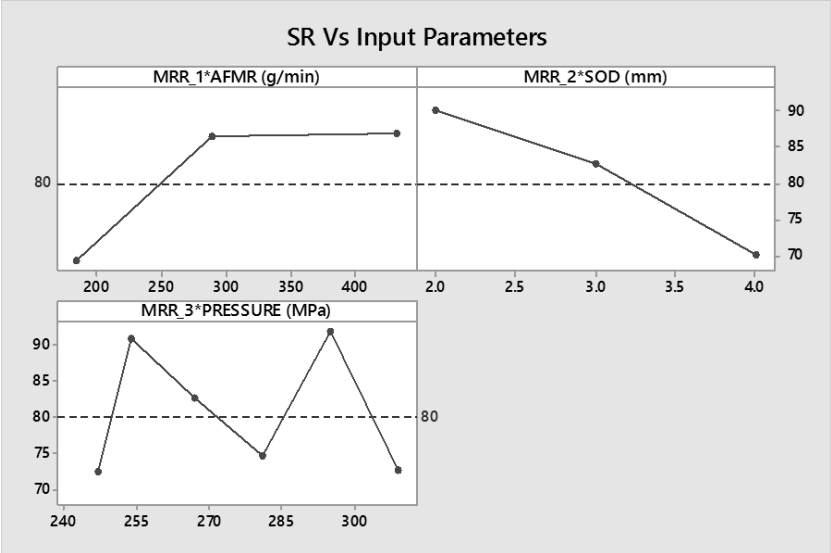

Fig. 7. MRR variations

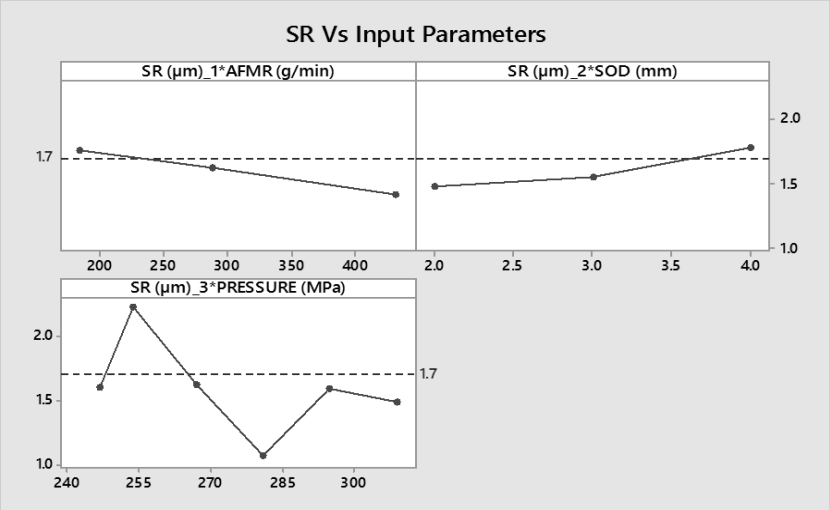

Fig. 8. Surface roughness variations

Table 10. Grey Relational Analysis

Input parameters	Level					
	1	2	3	4	5	6
Pressure	0.587554	0.436044	0.509623	**0.647716**	0.566758	0.561277
SOD	0.557775	**0.572099**	0.524613			
AFMR	**0.597603**	0.516078	0.540805			

5.6.2. Hole correction

Deep hole making in Brass consists of three stages. They are as indicated below:

The first stage Abrasive water jet impingement;

The second stage – Abrasive water jet penetration;

The third stage – Abrasive water jet dwell period.

Abrasive water jet impingement: In this stage the abrasive water jet creates an indent on the surface of the work piece. This stage decides the quality of the hole top surface.

Abrasive water jet penetration: in this stage the abrasive water jet penetrates along the depth of the work piece, removing the material till the bottom and comes out of the work piece, creating a tiny hole at the bottom, which is very small when compared to the top hole.

Abrasive water jet dwell: in this stage the abrasive water jet removes material at shallow angles and makes the hole bigger. It can also be referred as hole correction.

5.6.3. *Optimum hole profile*

The found optimal combination is used to make holes for finding the optimum hole correction time. As the hole penetration time is found to be 2 minutes 20 seconds for the predicted optimal combination, holes are made for 2 minutes 27 seconds, 2 minutes and 34 seconds and 2 minutes 40 seconds using the predicted optimal combination level of parameters. Then, the top and bottom diameters of the three holes are measured and kerf is calculated. The hole with minimum kerf occurred while machining for 2 minutes 40 seconds. Hole profiles of the particular hole is studied and is found to possess lesser standard deviation of the hole diameter with uniform hole profile. Hence, it is concluded that the hole correction time for deep hole making in brass at a depth of 50mm is 2 minutes and 40 seconds. The hole diameters of corrected holes are tabulated in Table 11.

The kerf angle of H20 is found to be minimum of all the holes. Moreover, the kerf angle tends to increase further. The hole profile of H20 is found to possess no barrel effect, convergence or divergence. Hence, it is called as a "Optimum Deep Hole in brass of 50mm length". The figure 12 shows the optimum deep hole profile.The optimal penetration time found in this study is 16 minutes and the hole correction time is 3 minutes. So a deep hole of 100mm length can be made in brass in a total time of 19 minutes with least deviation in their diameter throughout its depth.

Although deep holes can be made with least deviation in their diameter throughout its depth in brass, we have witnessed a barreling effect in the hole. i.e. the diameter of the hole gradually increases along its depth, until near center and gradually decreases from near center to bottom of the work piece. The reason for the barreling on top side is because the jet diameter increases as it reaches more depth i.e. the jet is narrower until certain depth and becomes wider thereafter. The reason for bottom barreling effect is because of less machining time (hole correction time). So the bottom barreling effect could be reduced by increasing the hole correction time, considering the large diameter in that hole as reference. The top barreling effect could be reduced by placing the same material of certain thickness on top of the work piece and machining holes could help reducing the barreling effect on top side.

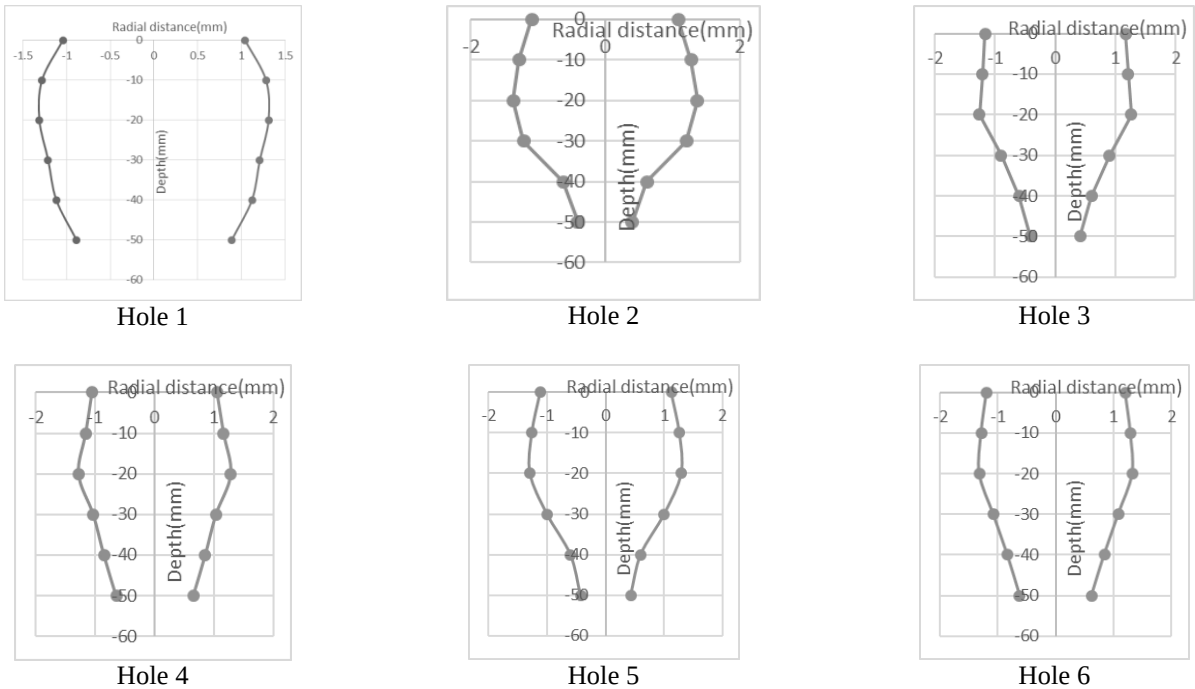

Hole 1 Hole 2 Hole 3

Hole 4 Hole 5 Hole 6

Fig. 9. Hole profiles (1-6)

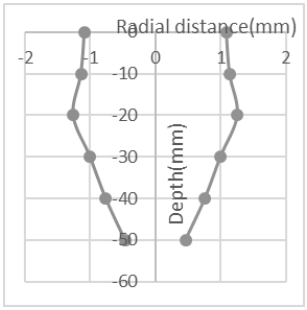

Hole 7

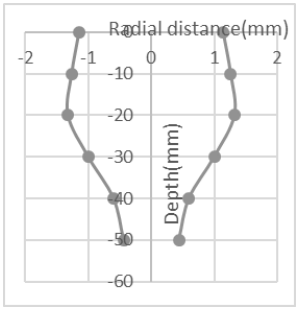

Hole 8

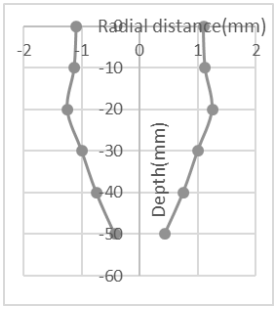

Hole 9

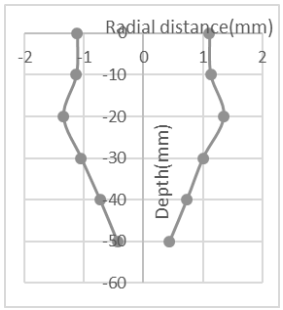

Hole 10

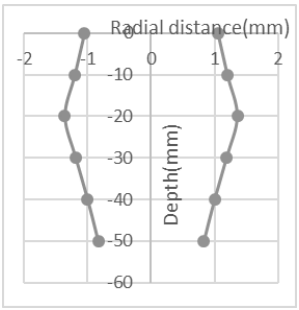

Hole 11

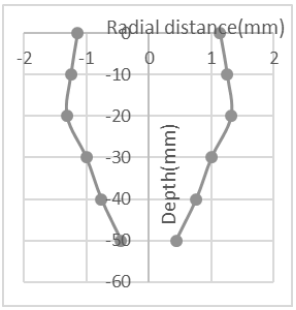

Hole 12

Fig. 10. Hole profiles (7-12)

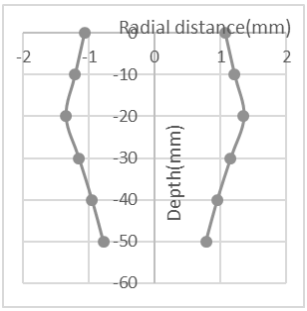

Hole 13

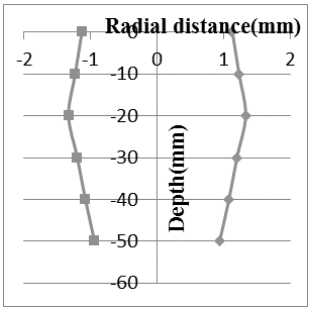

Hole 14

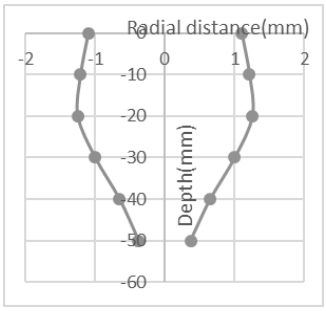

Hole 15

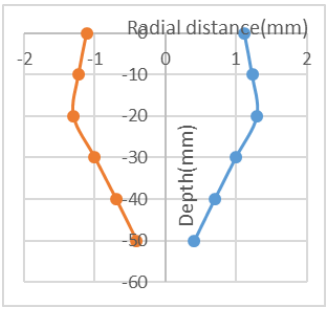

Hole 16

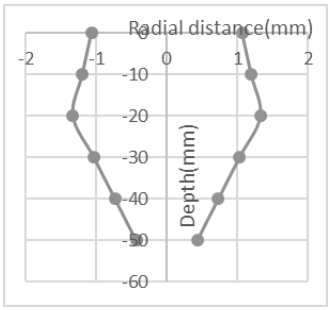

Hole 17

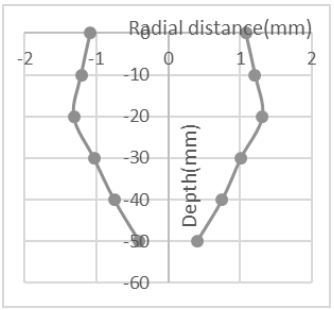

Hole 18

Fig. 9. Hole profiles (13-18)

Table 11. Diameter of Corrected Hole

Hole ID	Piercing Time	Top Diameter	Bottom Diameter	Kerf angle
H19	120s	2.243	1.0626	0.677
H20	127s	2.192	1.1423	0.602
H21	134s	2.3106	0.98	0.76
H22	140s	2.32	0.9923	0.762

6. CONCLUSIONS

In this study, deep holes of nominal diameter of 3 mm and length of 50 mm are made on brass and the effect of input parameters like pressure, stand-off distance and abrasive mass flow rate on hole quality are established. The Taguchi Orthogonal Design experiments are performed on brass with 6 levels for pressure, 3 levels each for SOD's and abrasive mass flow rate respectively. The penetration time is noted. The machined holes are sectioned into five parts of 10mm each and their depth average diameter (top and

bottom diameter) is measured and the standard deviation and range are calculated.

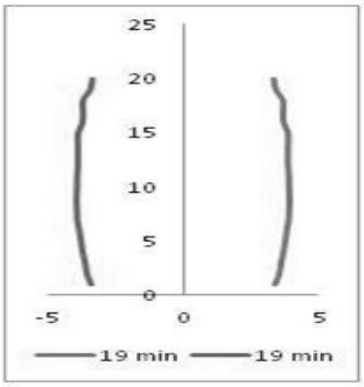

Fig. 12. Optimum deep hole profile

The input parameters are optimized for minimum SR, minimum Kerf Angle and maximum MRR in Minitab software, GRA and Taguchi Powered GRA and the effect of pressure, SOD and AMFR on hole quality are established. The predicted optimal combination of parameters are used to machine deep holes to find the hole correction time where the hole diameter is similar throughout its depth.

The Analysis of variance (ANOVA), F-test and Grey Relational Analysis are used to draw appropriate conclusions as follows:

- In machining deep holes on brass, the water pressure is the most significant factor on surface roughness, kerf angle and MRR;
- The recommended parametric combination for optimum hole quality i.e. minimum surface roughness, minimum kerf angle and minimum MRR Predicted from Minitab software, Grey Relational Analysis and Taguchi based GRA is AMFR (185 g/min), pressure (281 MPa), SOD (3 mm);
- The optimum hole penetration time and hole correction time are found to be 2 minutes 20 seconds and 2 minutes 40s respectively for making a deep hole of nominal diameter 3 mm and length 50 mm on brass.

Scope for future work:

- The pressure used in making deep holes can be increased and its effect on making deep holes can be studied;
- The abrasive type can be considered as another input parameter and its effect on making deep holes can be studied;
- The nozzle orifice size could be varied so that the hole size can be varied;
- A study can be done to reduce the barreling effect in making deep holes in brass;
- A study can be done to compare the barreling effect in various materials to find a relation for barreling effect vs machinability of the material;
- Minimization of standard deviation and range of the hole diameters can be done to obtain near perfect straight holes.

REFERENCES

1. Siores, E., Wong, W.C.K., Chen, L., Wager, J.G., (1996). *Enhancing Abrasive Waterjet cutting of Ceramics by Head Oscillation Techniques*, Annals of the CIRP, 45(1), 327-300.

2. Momber, A., Kovacevic, R., (1998). *Principles of Abrasive Waterjet Machining*, Springer-Verlag, London.

3. Wang, J, Guo, DM, (2002). *A predictive depth of penetration model for abrasive waterjet cutting of polymer matrix composites*, J Mater Process Technol, 121(2-3), 390-394.

4. Axinte, DA, Karpuschewski, B, Kong, MC, Beaucamp, AT, Anwar, S, Miller, D, Petzel, M, (2014). *High Energy Fluid Jet Machining (HEFJet-Mach): from scientific and technological advances to niche industrial applications*, CIRP Ann Manuf Technol, 63(2): 751-771.

5. Chitirai Pon Selvan, M., Mohanasundara Raju, N., (2012). *A study of surface roughness in AWJ cutting of mild steel*, Ind. J. Mech. Prod. Eng. Res. Development., 2(3), 10-18.

6. Chitirai Pon Selvan, M., Mohanasundara Raju, N., (2012). *Influence of AWJ cutting conditions on depth of cut of mild steel*, Int. J. Des. Manu. Tech., 3(1), 48-57.

7. Thakkat., K.H., Vipul.M.Prajapati, V.M., Thakkar, S.A., (2013). *A Machinability study of Mild Steel using AWJM Technology*, J. Eng. Res. Appl., 3(3), 1063-1066.

8. Liu, H.T., (2007). *Hole drilling with abrasive fluid jets*, Int. J. Adv. Manuf. Tech., 32, 942–957.

9. Palleda, M., (2007). *A study of taper angles and material removal rates of drilled holes in AWJM process*, J. Mater. Process. Tech., 189, 292–295.

10.Kurt, M., Hartomacioglu, S., Mutlu, B., Koklu, U., (2012). *Minimization of the surface roughness and form error on the milling of free-form surfaces using a Grey Relational Analysis*, Materials and technology, 3, 205-213.

11.Pandey, N., Pal, V., Katiyar, J.Kr., (2012). *Investigation of drilling time V/S material thickness using AWJM*, Int. J. Adv. Eng. Tech., 4(1), 672-678.

12.NPTEL, *Design for reliability and quality*, IIT, Bombay.

13.Venkata Rao, K., Murthy, B.S.N., Mohan Rao, N., (2013). *Cutting tool condition monitoring by analyzing surface roughness, work piece vibration and volume of metal removed for AISI 1040 steel in boring*, Measurement, 46(10), 4075 – 4084.

14.Gupta,V., Pandey, P.M., Pal Garg, M., Khanna, R., Batra, N.K., (2014). *Minimization of kerf taper angle and kerf width using Taguchi's method in abrasive water jet machining of marble*, Procedia Materials Science, 6, 140 – 149.

Received: December 10, 2017 / Accepted: June 15, 2018 / Paper available online: June 20, 2018